Square-Array Direct-Current Resistivity Measurements Conducted at Nye County near Borehole NC-EWDP-29P

Abstract

Azimuthal square-array direct-current resistivity soundings were used to determine the presence and azimuth of fractures in volcanic tuffs at a location near the southwest corner of the Nevada Test Site in Nye County, Nevada. The units underlie approximately 100 meters of alluvium at the investigation site. The feasibility of the square-array resistivity soundings to resolve the contact between alluvium and tuff also was tested. Results of the soundings indicate that a fracture zone exists within the tuff and has a predominant strike direction of approximately N. 30º to 45º E. to N. 60º to 75º E. Results also indicate that the relatively thick sequence of alluvial sediments at this site makes the contact between the alluvium and the tuff difficult to resolve using this method.

Introduction

During the spring of 2005, the U. S. Geological Survey (USGS) conducted square-array direct-current resistivity (SAR) measurements at a site near borehole NC-EWDP-29P. This approach is similar to other one-dimensional electrical resistivity sounding methods. Reported applications of this approach have shown the method to be effective in characterizing fracture orientation in shallow bedrock environments (Lane and others, 1995; Bills and others, 2000). The purpose of this work was to test the feasibility of the square array resistivity method to delineate subsurface fractures in areas where relatively thick alluvial deposits are known to occur. The utility of the method to determine the contact between the alluvium and the volcanic tuffs also was tested. Assuming an isotropically resistive alluvial overburden, it was hypothesized that the contact between the alluvium and the fractured volcanic tuffs could be determined. The motivation behind this work was related to concerns that fractures could provide offsite migration pathways for the transport of radionuclides from the proposed Yucca Mountain nuclear waste repository.

The work reported here represents a substantial effort on the part of the USGS and the Nye County Nuclear Waste Repository Project Office. This effort has led to the collection of a large and detailed data set. The data analysis and interpretation have been performed to illustrate the utility of the SAR method in environments that are characterized by thick alluvial deposits. However, it is beyond the scope of the project to conduct more in-depth analyses such as incorporating dipping beds and in-depth interpretations such as using advanced modeling methods to help identify correlations of SAR derived apparent resistivity values and specific tuff lithologies.

Acknowledgements

Appreciation is extended to the Nye County Nuclear Waste Repository Project Office for funding and providing field support for this work. In particular, Dr. Dale Hammermeister and Jamieson Walker were instrumental in the success of this effort. Nye County contractors and staff including Rocky Rockwood, Ed Huskinson, Doug Davis, and Levi Kryder provided logistical support and essential assistance in field operations.

Square-Array Method

Resistivity is a measure of a materials resistance to the flow of electrical current. Field measurements result in apparent resistivity (ρ_a) values that are generally related to rock type and water content, which is often related to grain-size distribution; finer grained materials typically have higher water content than coarse grained materials and consolidated rock. The values also are affected by the location and spacing of the electrode array, which determines the sample volume of the measurement; the larger the electrode spacing, the larger the sample volume (sample depth). In addition, if the electrical properties of the media vary with direction (anisotropic), then the apparent resistivity can also be dependent on the azimuth of the array. In horizontally stratified systems the plane of anisotropy is generally parallel to the surface. In dipping layered rock units, the plane of anisotropy is not parallel to the surface and, the measured apparent resistivity will be dependent on orientation. This situation also applies to fractured rock units such as those thought to occur at this site.

The SAR technique (Habberjam and Watkins, 1967) was used to determine the presence and azimuth of subsurface fracture zones in the volcanic tuff. Using the SAR method, the azimuth of existing fracture zones is generally indicated by a decrease in resistivity along a particular azimuth relative to other azimuths.

SAR measurements are obtained in a manner similar to that for collinear arrays used in resistivity sounding measurements where current is applied to two current or transmitter electrodes (A and B; fig. 1) and the potential measurements are made at two potential or receiver electrodes (M and N). Data obtained from these measurements can be used to derive one-dimensional plots of the apparent resistivity distribution as a function of depth. However, unlike collinear arrays, the electrodes for the square array are placed at the corners of a square having sides of length *a*. In this manner the electrode spacing (*a*-spacing) becomes the length of the side of the square (*a*) and the location of the measurement point is assigned to the center of the square. The depth of investigation can generally be considered approximately equal to the length of the side of the square but varies with resistivity.

Using this geometry, three resistivity measurements are made; two perpendicular measurements (alpha, $\rho_{a\alpha}$; and beta, $\rho_{a\beta}$) and one diagonal measurement (gamma, $\rho_{a\gamma}$) (fig. 1a). The azimuth of the $\rho_{a\alpha}$ and $\rho_{a\beta}$ measurements is represented by the line connecting the current electrodes (A and B). The $\rho_{a\gamma}$ measurement provides a check on the accuracy of the $\rho_{a\alpha}$ and $\rho_{a\beta}$ measurements. In a homogeneous isotropic medium,

$$\rho_{a\gamma} = 0, \text{ therefore, } \rho_{a\alpha} = \rho_{a\beta}, \qquad \text{and}$$

in a homogeneous anisotropic medium,

$$\rho_{a\gamma} = \rho_{a\alpha} - \rho_{a\beta}.$$

After making these three measurements, the array is expanded symmetrically about the center, usually in increments of $a\sqrt{2}$, so that the soundings can be interpreted as a function of depth.

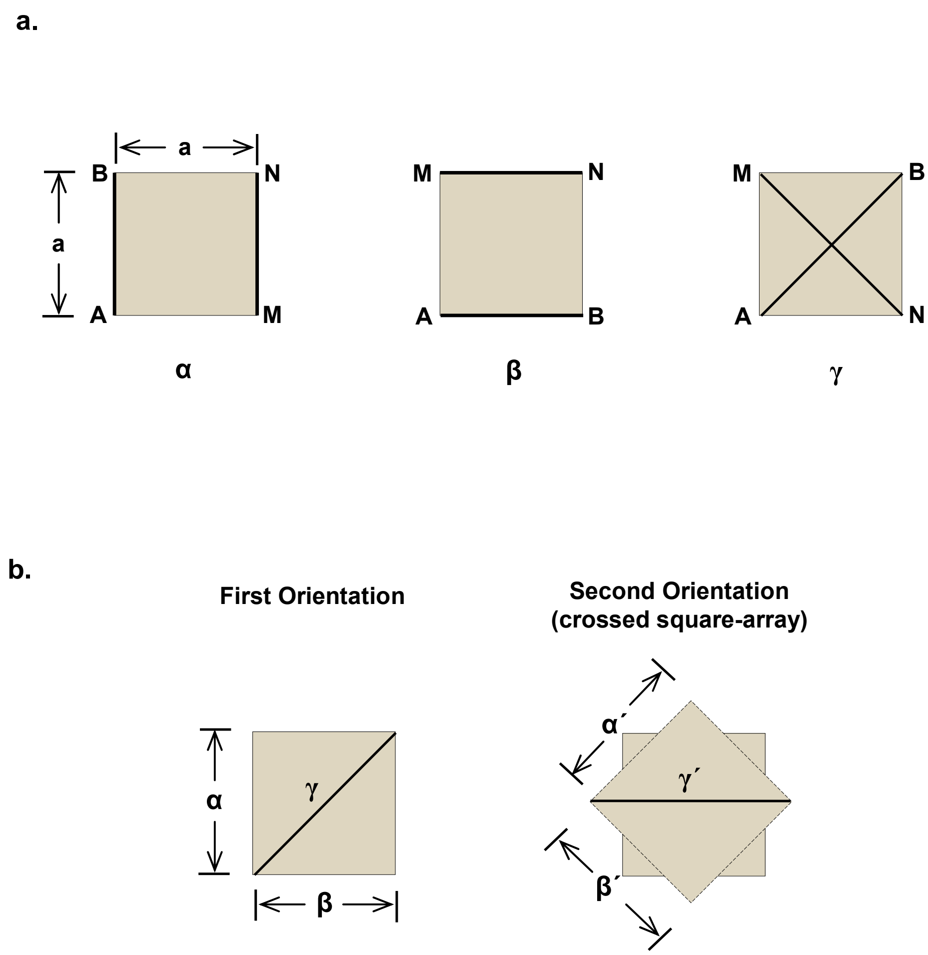

Figure 1. (a) Electrode configurations for each square array; AB = current electrodes, MN = potential electrodes. (b) Crossed arrays: second orientation is rotated 45 degrees about the center point.

Apparent resistivity values are obtained from the following relation:

$$\rho_a = \frac{K\Delta V}{I}$$

where: ρ_a = the apparent resistivity, in ohm-meters;
K = the geometric factor for the array;
ΔV = the measured potential difference between electrodes M and N, in volts; and
I = the applied current, in amperes.

For the square array, the geometric factor is given by,

$$K = \frac{2\pi a}{2 - \sqrt{2}}, \quad \text{(Habberjam and Watkins, 1967)}$$

where *a* = the square-array side length, in meters.

Once the largest square measurements are made, the square is collapsed, rotated 15º, and expanded again. For the work that is reported here, six complete expansions separated by 15º rotations were performed, thus yielding measurements of apparent resistivity along 12 directions. This provided sufficient data for graphical display and interpretation as well as three independent crossed square-array data sets (i.e., data sets separated by 45º, fig.1b) that could be used for analytical analysis of the results. The graphical display is mirrored on polar coordinates to yield a 360 degree plot (fig. 2a). The usefulness of this method relies on azimuthal resistivity differences related to the predominant structural orientation of fractures. Assuming that fractures in the tuff are oriented in predominantly one direction, resistivity will be lower in the direction of the fractures. This anisotropic-resistivity will manifest as a resistivity ellipse in polar coordinate plots (fig. 2b). The azimuth of the minor axis of the resistivity ellipse is inferred to be the predominant azimuth of the fracture zones in the tuff.

Lithology of Borehole NC-EWDP-29P and Initial Assumptions of Investigation

The lithologic log from borehole NC-EWDP-29P at this site indicates that about 98 m of alluvium overlies the Tiva Canyon Tuff. The alluvium is described in three intervals; an upper interval consisting of layers of well graded sand with silt, clay, and gravel to a depth of about 38 m; a middle interval consisting of weakly to moderately cemented thick layers of interbedded silty, clayey sand with gravel and well-graded sand with silt, clay and gravel to a depth of about 81 m, and a lower interval which consists of a uniform sequence of silty, clayey sand with gravel. Particle size data obtained from Nye County staff shows that there is a general and gradual trend of increasing fines with depth (Nye County, written commun., 2005).

Initial assumptions of this investigation were that the resistivity contrast between the alluvium and tuff is sufficient to allow for the determination of the alluvium/tuff contact and, that a relatively isotropically resistive alluvium is underlain by an anisotropically resistive tuff. Under the assumption that the depth of investigation is

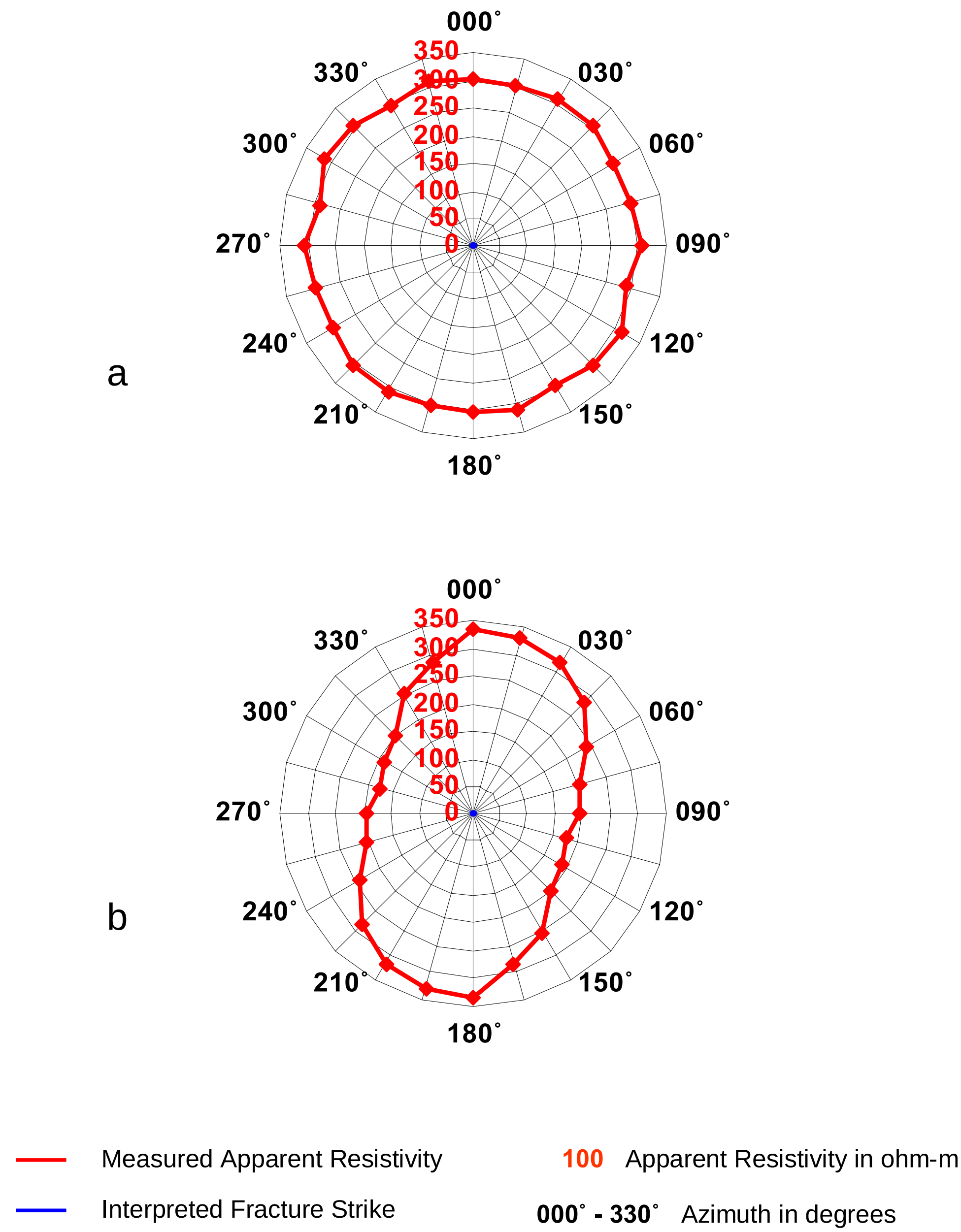

Figure 2. Hypothetical azimuthal plots of apparent resistivity showing (a) the uniform circular plot for a homogeneous isotropic half-space, and (b) ellipsoid plot for a homogeneous anisotropic half-space. The minor axis of the ellipse (predominant fracture strike) would lie along the 285º - 105º azimuth.

approximately equal to the *a*-spacing, it was anticipated that the greatest change in resistivity would occur between measurements at *a*-spacings less than and greater than about 98 m. The anticipated resistivity response that marks the beginning of anisotropically resistive conditions would be used to aid in the determination of the alluvial thickness. The lithologic log also indicates that depth to water at this site is about 110 m below land surface, thus it was anticipated that a reduction in overall resistivity could occur for *a*-spacings of about 110 m and greater.

Results

Graphical interpretation of fracture azimuths

For each square-array orientation, measurements were obtained for *a*-spacings that ranged from 2.8 to 1,448.2 m. The results of these measurements were used to make a total of 342 apparent resistivity determinations. Plots were graphically analyzed for each *a*-spacing in polar coordinates to determine the presence or absence of a resistivity ellipse resulting from anisotropy (figs. 3a-s). Predominant fracture strike orientations were interpreted subjectively as being 90 degrees from the direction of maximum observed apparent resistivity.

Results indicate relatively isotropic resistivity conditions for *a*-spacings between 2.8 to 22.6 m (fig. 3a-g). Apparent resistivity values for these *a*-spacings generally decreases from about 400 ohm-m at shallow depths to 250 ohm-m at greater depths. Anisotropic conditions begin to become apparent at an *a*-spacing of 33.9 m where the minor axis of the ellipse is about 225 ohm-m and the major axis is about 300 ohm-m (fig. 3h). Apparent resistivity values continue to decline slightly with increasing *a*-spacing and the general shape of the ellipse is consistent out to an *a*-spacing of 67.9 m (fig. 3j). The ellipsoidal shape of the apparent resistivity plots for *a*-spacings between 33.9 m and 67.9 m are interpreted as being the result of anisotropy in the middle and lower units of the alluvium. Each of the ellipses has a minor axis oriented about N. 30° to 40° E.

For *a*-spacings of 90.5 meters and beyond, the resistivity ellipse is more pronounced and somewhat irregular (fig. 3k-p). For these *a*-spacings it is expected that the minor axis of the ellipse coincides with the azimuth of the major fracture orientation in the tuff. The minor axis of the ellipse for these measurements also are about N. 30° to 45° E. These plots also show that reduced apparent resistivities occur along azimuths between N. 60° to 75° E. The irregular pattern of the resistivity ellipses could be attributed to multiple fracture zones, poor signal, or a combination of these. Due to diminished signal strength, apparent resistivity values for orientations at *a*-spacings beyond 724.1 m could not always be as reliably determined (figs. 3q-s).

Crossed square-array analysis

A more quantitative (anisotropic analysis) approach to determine the fracture strike (Habberjam, 1975) was also attempted. This approach relies on an analysis of the crossed square-array data. The results of this analysis were inconclusive and are attributed mainly to the thick overburden (> 100 m) at this site.

Equivalent Wenner array sounding curve

Measured square array apparent-resistivity data were transformed to an equivalent collinear Wenner array sounding curve that was interpreted using standard methods. This was accomplished by reducing the square array measurements to a set of directionally independent apparent resistivity values given by

$$\rho_m = \left[(\rho_{a\alpha})(\rho_{a\beta})\right]^{1/2}, \qquad \text{(Habberjam and Watkins, 1972)}$$

where ρ_m is the mean geometric apparent resistivity. The resulting mean geometric apparent resistivity values can be plotted as a function of an equivalent collinear Wenner array electrode separation to produce a 1-D sounding curve. Among the common collinear arrays used in resistivity measurements, the Wenner array provides the greatest sensitivity to vertical changes in subsurface resistivity. These data were inverted using a least-squares optimization procedure to produce a 1-D layered earth model (fig. 4).

The results of this analysis show that an apparent resistivity low occurs along a depth interval that extends from approximately 100 to 200 m. The resistivity low is interpreted as the result of the presence of the water table and the associated saturated conditions that exist in the tuff. Despite the increased sensitivity to vertical changes in subsurface resistivity in Wenner array soundings, the presence of the water table near the alluvium/tuff contact complicates the ability to discriminate the changes in resistivity that might otherwise be due only to changes is lithology.

Summary

Square array resistivity measurements were made in Nye County, Nevada at the Nye County Early Warning Drilling Program borehole NC-EWPD-29P. Measurements were made resulting in a total of 342 apparent resistivities. Graphical interpretation indicates that the predominant fracture azimuth for the Tiva Canyon Tuff is approximately N. 30º to 45º E., with possible secondary fracturing along N. 60º to 75º E. The predominant fracture azimuth generally did not change with increasing depth. An equivalent Wenner array sounding curve analysis for the site correlates well with the known depth to water.

The initial assumption of isotropically resistive alluvium was incorrect. Without the aid of a lithologic log, this incorrect assumption could have resulted in an underestimation of depth to the alluvium/tuff contact. For this reason, the SAR method alone would not be, in general, the ideal method for resolving the alluvium/tuff contact. Conventional collinear Wenner or Schlumberger array resistivity methods would instead be a better choice. Additional square array surveys in the area, however, could be helpful in better defining the anisotropic nature of the middle and deeper alluvial units and contrasting them with the underlying tuff.

From this work, it appears that in settings where thick anisotropic alluvial units are known to exist, the efficacy of the SAR method for determining fracture strike would be enhanced when additional site specific information (i.e., depth to bedrock) is available thus allowing greater confidence in the interpretations. Without prior knowledge regarding the depth to bedrock, anisotropic conditions that may exist in the alluvium could be interpreted as fracture or bedding strike in the target rock units.

References

Bills, D.J., Truini, M., Flynn, M.E., Pierce, H.A., Catchings, R.D., and Rymer, M.J., 2000, Hydrogeology of the regional aquifer near Flagstaff, Arizona, 1994-97: U.S. Geological Survey Water-Resources Investigations Report 00—4122, 143 p.

Lane, J.W., Jr., Haeni, F.P., and Watson, W.M., 1995, Use of square-array direct-current resistivity methods to detect fractures in crystalline bedrock in New Hampshire: Groundwater, v. 33, no. 3, p. 476-485.

Habberjam, G.M., 1975, Apparent resistivity, anisotropy and strike measurements: Geophysical Prospecting, v. 23, no. 2, p. 211-247.

Habberjam, G.M., 1972, The effects of anisotropy on square array resistivity measurements: Geophysical Prospecting, v. 20, no.2, p. 249-266.

Habberjam, G.M., and Watkins, G.E., 1967, The use of a square configuration in resistivity prospecting: Geophysical Prospecting, v. 15, no. 3, p. 445-467.

Figure 3. Azimuthal plots of square array resistivity measurements for different *a*-spacings.

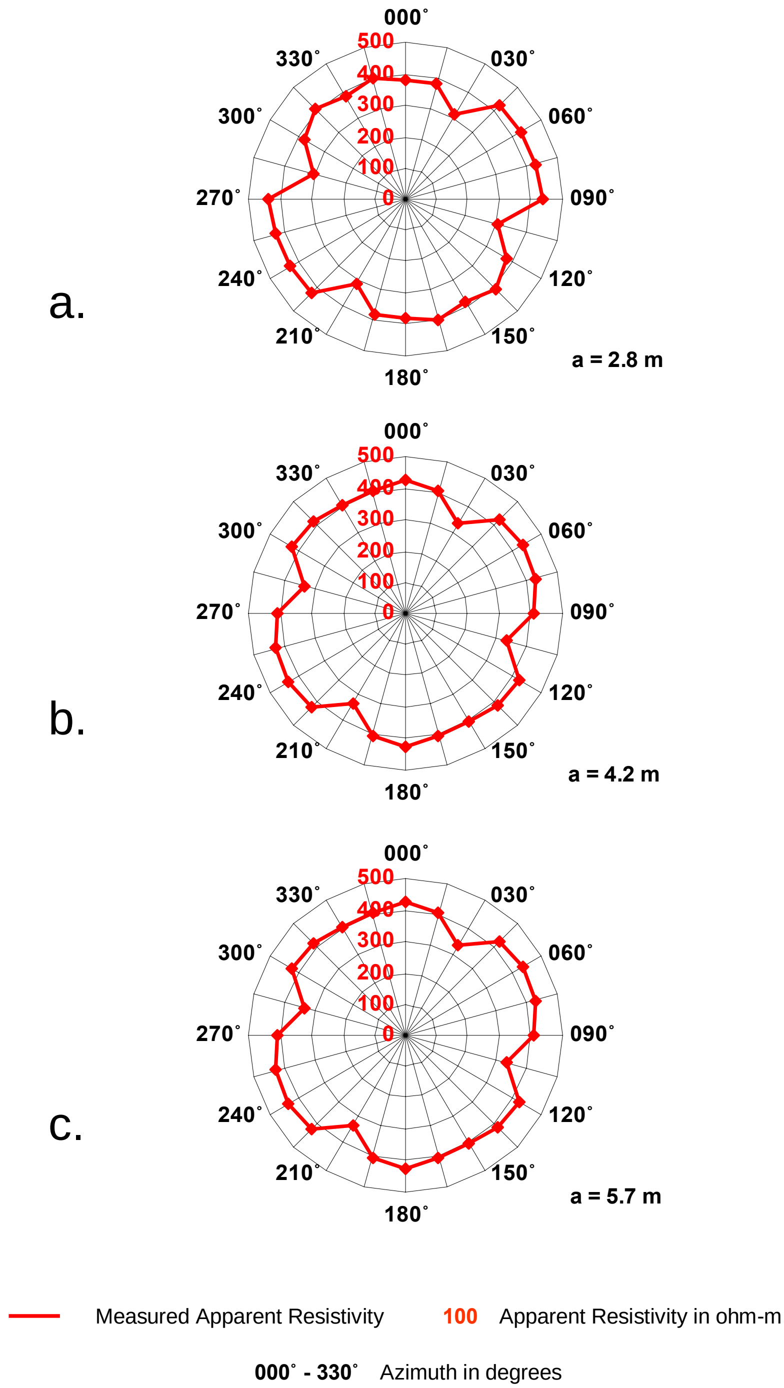

d.

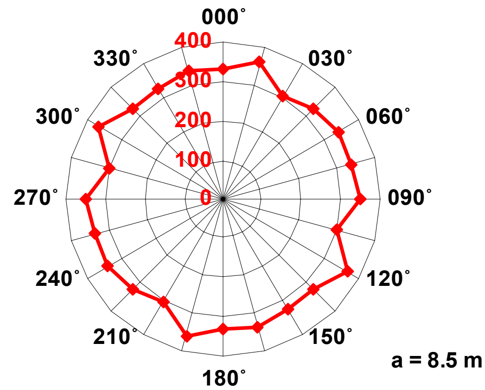

e.

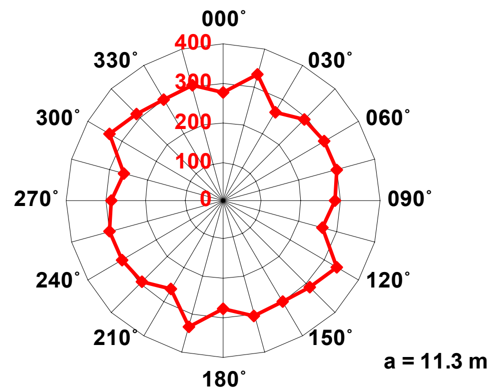

f.

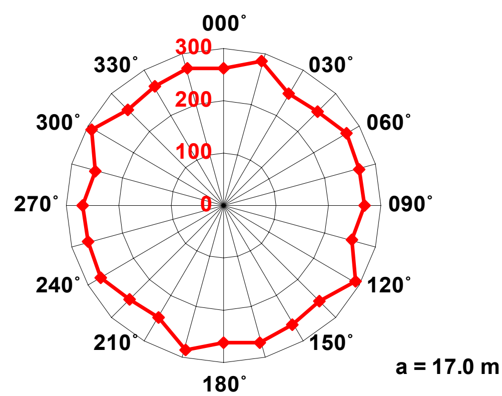

Measured Apparent Resistivity **100** Apparent Resistivity in ohm-m

000˚ - 330˚ Azimuth in degrees

g.

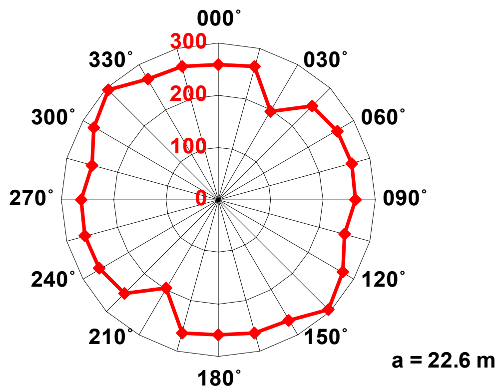

h.

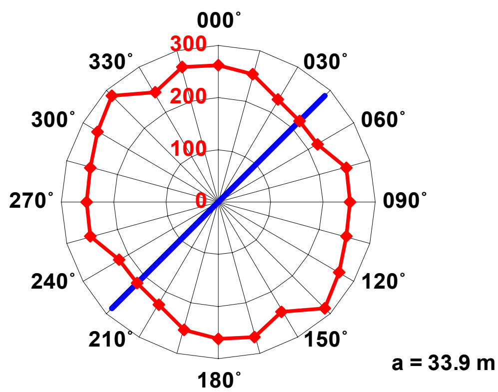

i.

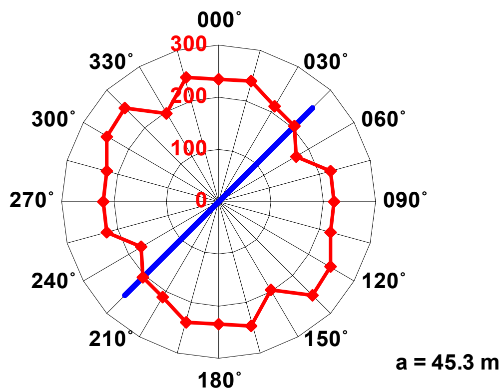

Measured Apparent Resistivity

100 Apparent Resistivity in ohm-m

Interpreted Fracture Strike

000˚ - 330˚ Azimuth in degrees

j.

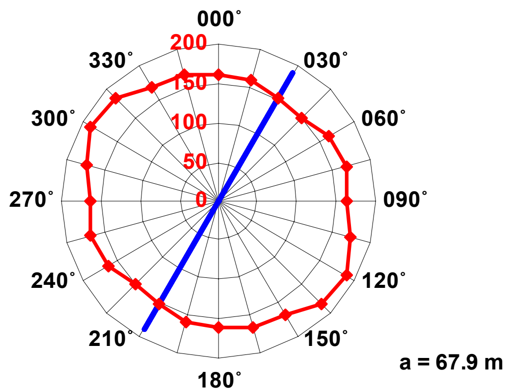

k.

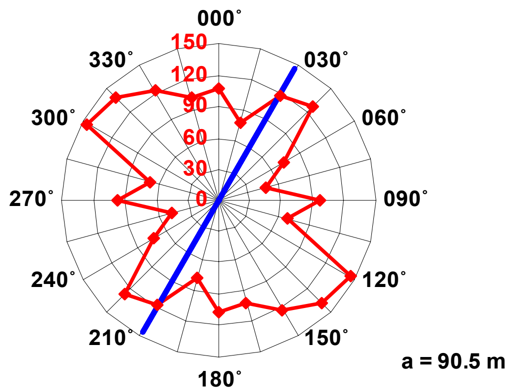

l.

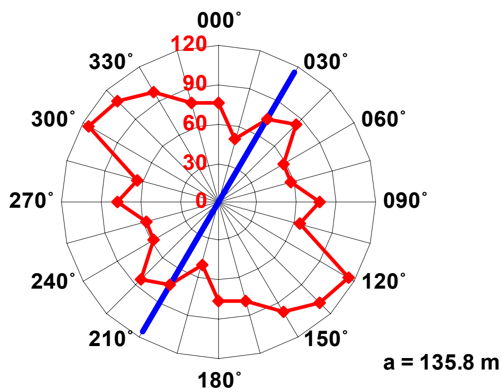

Measured Apparent Resistivity — **100** Apparent Resistivity in ohm-m

Interpreted Fracture Strike — **000˚ - 330˚** Azimuth in degrees m.

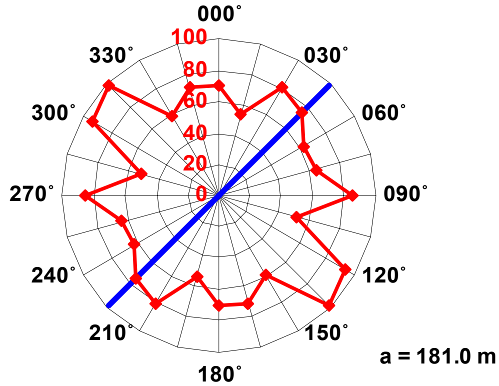

n.

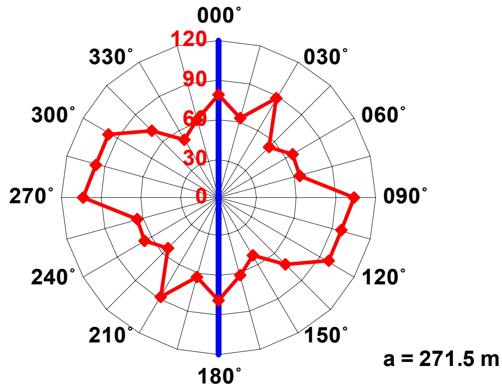

o.

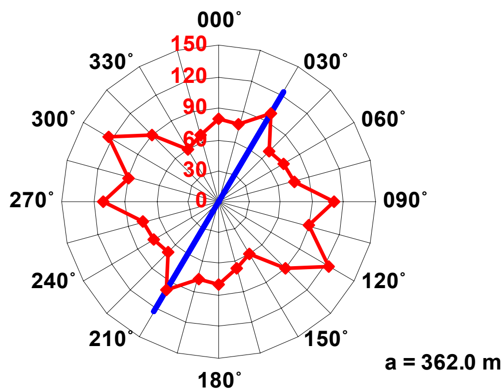

Measured Apparent Resistivity **100** Apparent Resistivity in ohm-m

Interpreted Fracture Strike **000˚ - 330˚** Azimuth in degrees p.

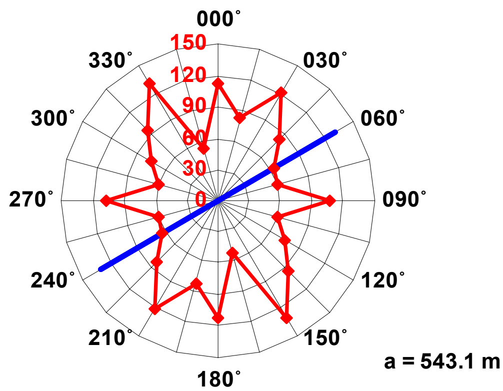

q.

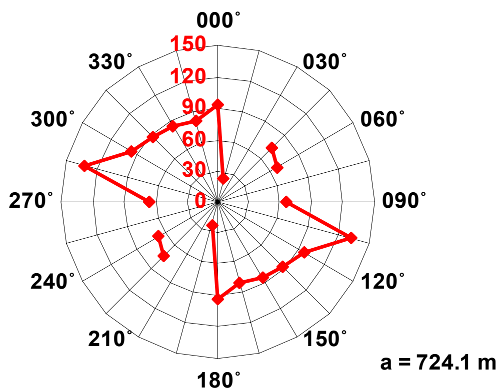

r.

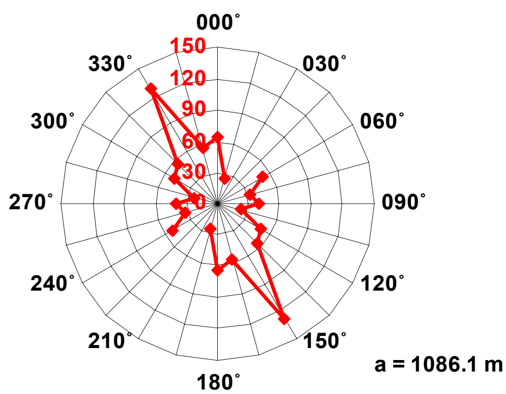

Measured Apparent Resistivity   120 Apparent Resistivity in ohm-m

Interpreted Fracture Strike   000° - 330° Azimuth in degrees

S.

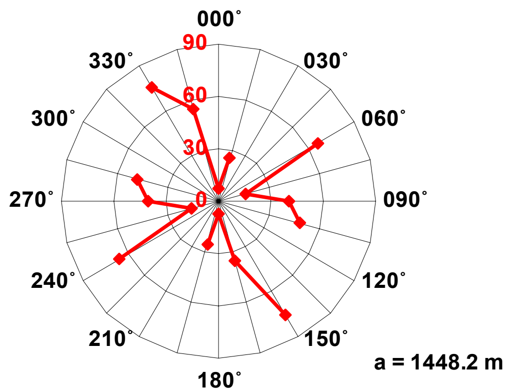

Measured Apparent Resistivity **100** Apparent Resistivity in ohm-m

000˚ - 330˚ Azimuth in degrees

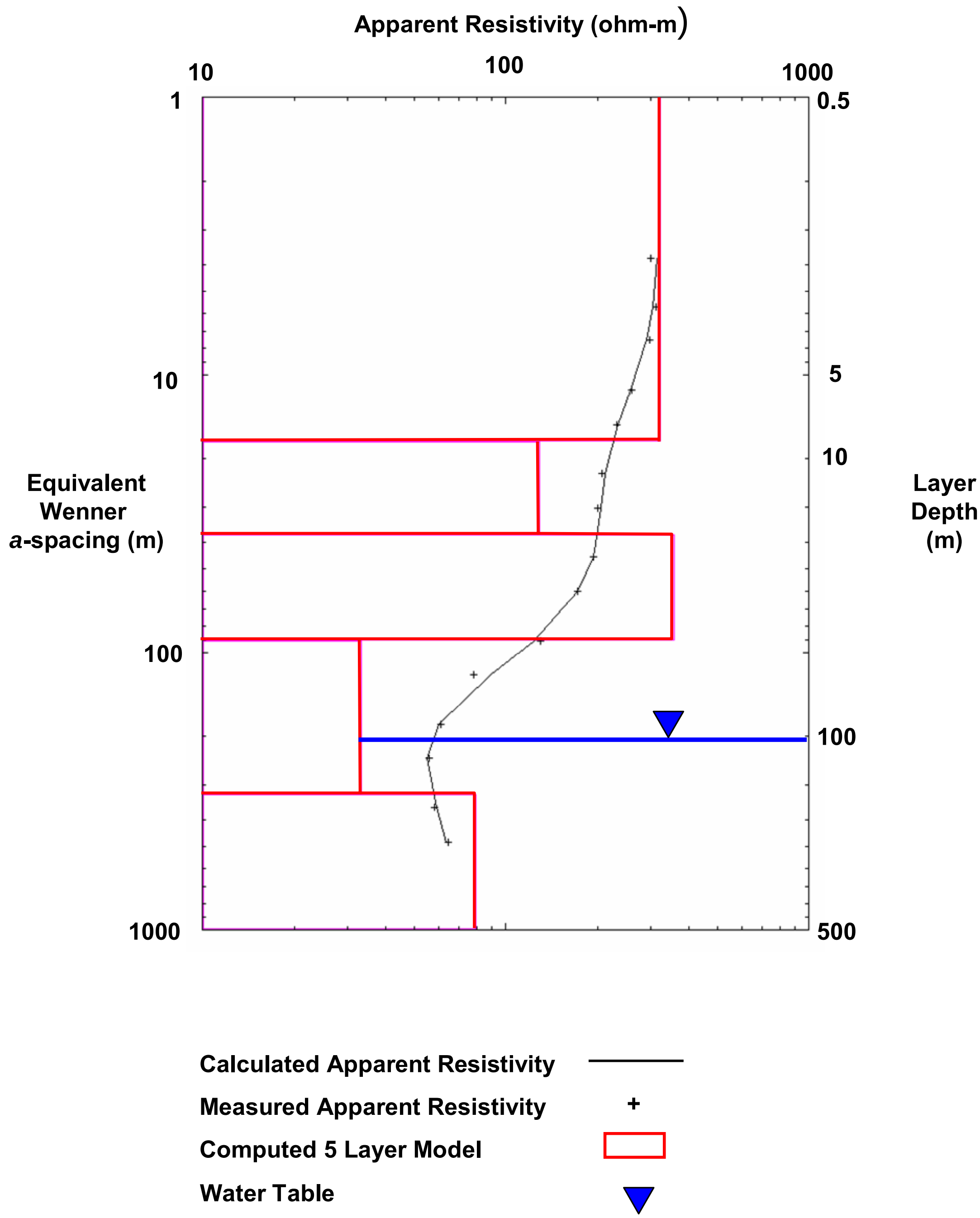

Figure 4. Equivalent Wenner array sounding curve and simulated 1-D layered earth model. Note that the depth scale for model layers is the right vertical scale.